Title

Ligand-Directed Actinide Oxo-Bond Manipulation in Actinyl Thiacalix[4]arene Complexes

Authors

Arnold, Polly Louise
Pyrch, Mikaela M
Meyer, Rachel L
et al.

Publication Date

2025-01-21

DOI

10.1002/anie.202422974

Peer reviewed

How to cite: Angew. Chem. Int. Ed. 2025, e202422974
doi.org/10.1002/anie.202422974

Actinides

Ligand-Directed Actinide Oxo-Bond Manipulation in Actinyl Thiacalix[4]arene Complexes

*Mikaela M. Pyrch, Rachel L. Meyer, Thayalan Rajeshkumar, Piper A. Cooke, David J. Fiszbein, Emi Ito, Nicholas J. Katzer, Cambell S. Conour, Stefan G. Minasian, Laurent Maron, and Polly L. Arnold.**

Abstract: Understanding the chemistry of the inert actinide oxo bond in actinyl ions AnO_2^{2+} is important for controlling actinide behavior in the environment, during separations, and in nuclear waste (An=U, Np, Pu). The thioether calixarene TC4A (4-*tert*-butyltetrathiacalix[4]arene) binds equatorially to the actinyl cation forming a conical pocket that differentiates the two *trans*-oxo groups. The 'ate' complexes, $[A]_2[UO_2(TC4A)]$ ($A=[Li(DME)_2]$, $HNEt_3$) and $[HNEt_3]_2[AnO_2(TC4A)]$ (An = U, Np, Pu), enable selective oxo chemistry. Silylation of the U^{VI} oxo groups by bis(trimethylsilyl)pyrazine occurs first at only the unencapsulated *exo* oxo and only one silylation is needed to enable migration of the *endo* oxo out of the cone, whereupon a second silylation affords the stable U^{IV} *cis*-bis(siloxide) $[A]_2[U(OSiMe_3)_2(TC4A)]$. Calculations confirm that only one silylation event is needed to initiate oxo rearrangement, and that the putative *cis* dioxo isomer of $[UO_2(TC4A)]^{2-}$ would be stable if it could be accessed synthetically, at only 23 kcal.mol^{-1} in energy above the classical *trans* dioxo. Calculations for the transuranic *cis*$[AnO_2(TC4A)]^{2-}$ (An=Np, Pu) are at higher energies, 30–35 kcal.mol^{-1}, retaining the U complexes as the more obvious target for a *cis*-dioxo actinyl ion. The aryloxide (OAr) groups of the macrocycle are essential in stabilizing this as-yet unseen uranyl geometry as further bonding in the TC4A U-O_{Ar} groups stabilizes the U=O 'yl' bonds, explaining the stability of the putative *cis*$[UO_2(TC4A)]^{2-}$ in this ligand framework.

[*] Dr. M. M. Pyrch, Dr. R. L. Meyer, P. A. Cooke, D. J. Fiszbein, E. Ito, N. J. Katzer, C. S. Conour, Prof. P. L. Arnold.
College of Chemistry, University of California Berkeley, Berkeley, California 94720, USA

Dr. M. M. Pyrch, Dr. R. L. Meyer, P. A. Cooke, D. J. Fiszbein, N. J. Katzer, C. S. Conour, Dr. S. G. Minasian, Prof. P. L. Arnold.
Chemical Science Division, Lawrence Berkeley National Laboratory, Berkeley, California 94720, USA
E-mail: pla@berkeley.edu

T. Rajeshkumar, Prof. L. Maron
LPCNO Université de Toulouse, INSA Toulouse, 135 Avenue de Rangueil, 31077 Toulouse, France

Introduction

The uranyl(VI) dication $[UO_2]^{2+}$ is the most common form of uranium in the environment, and is reduced by minerals and microbes to the less stable uranyl(V) monocation $[UO_2]^{+}$ and then beyond to stable, less environmentally mobile U(IV) phases.[1] Over the last decade significant progress has been made in understanding the reduction and oxo-functionalization of $[UO_2]^{2+}$.[2] This is important as reduction processes limit the environmental spread of the otherwise mobile actinyl dication by forming immobile reduced phases.[2e,3] Around 98 percent of the actinide content in processing solutions of spent nuclear fuel takes the form of linear actinyl ions of U, Np, and Pu that have strong actinide oxygen multiple bonding, and their oxo group chemistry can cause problems of clustering and precipitation in the manipulations. Meanwhile, actinyl oxo group silylation and reduction also offers an excellent opportunity to explore covalency in An–O bonding.[4] Rigorous anaerobic reaction conditions along with strategic ligand design have allowed this research field to flourish in the past decade, and a variety of strategies have been employed to achieve functionalization of the uranyl oxo, alongside as-yet unsuccessful efforts to displace the *trans* oxos into a *cis* geometry,[5] which would be a fascinating target for bonding studies. The *cis* geometry, which would be expected for a d-block analogue, has been theoretically predicted, but not yet experimentally observed.[6–8] With this aim, the use of H-bond donors and/or auxiliary metal cations binding to one oxo, in order to facilitate oxo group functionalization at the secondary oxo has been explored,[3b,9] and the binding of a Lewis acid such as a borane to the uranyl oxo group also used to lower the actinyl ion's reduction potential.[10] Our group and others have explicitly designed ligand scaffolds to enforce the interaction of uranyl with H-bond donors and auxiliary metals;[2e,11] these close interactions in conjunction with the ligand frameworks have so far generated interesting uranyl oxo reactivity, including oxo migration, complete deoxygenation, and formation of bridging species.[2a,10a,11c,12,13]

Here, we sought to explore the use of added Lewis acids to control the chemistry of the two actinyl oxo groups that are differentiated by the conically shaped 4-*tert*-butyltetrathiacalix[4]arene (TC4A) ligand, a known chelator for uranyl, Figure 1.[14] Our previous designs used two pyrroles as H-bond donors for one oxo in a folded, octa-aza

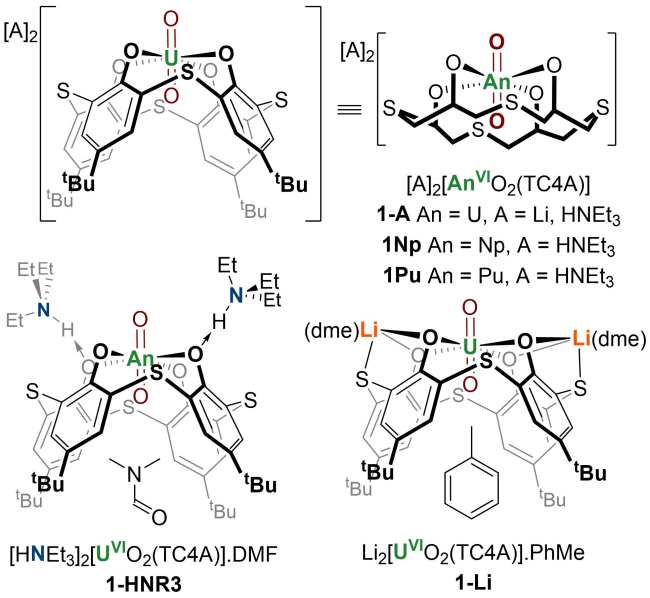

Figure 1. An abbreviated cartoon drawing of **1-A** (A=Li, $HNEt_3$), **1Np**, **1Pu**, and drawings of the solid-state structures of **1** that show the position of the lattice solvent. (The U^{VI} congener **1-HNR3** is a literature complex.)[14a]

macrocyclic uranyl complex to desymmetrize the uranyl ion.[3b] In the TC4A framework, neither oxo is directly H-bonded, so both are chemically accessible, and the An^{VI} actinyl complex is now dianionic, enabling the docking of a variety of cations and H-bond donors to the uranyl complex that can either protect its reactivity or adjust the electron-richness of the metal oxo groups.[3a,15]

The mild reductive silylation reagent bis(trimethylsilyl)pyrazine, $(Me_3Si)_2pyz$ is a source of the $Me_3Si^{\bullet}$ radical and used widely for metal halide reduction, as well as recently for the reductive functionalization of the uranyl oxo group.[16] Herein, we report differences in the silylation behavior of a set of 'ate' complexes of the uranyl cation $[A]_2[UO_2(TC4A)]$ (A = [Li(DME)], $HNEt_3$), in the thioether – expanded calixarene TC4A, through a combination of experiment and theory. We show how the reduction associated with silylation allows the migration of the oxo groups, and the role the counter-cations play by forming additional interactions with the calix – O atoms that help the rearrangement and subsequent silylation, and assess the possibility of generating the as-yet unobserved *cis*-dioxo actinyl (U, Np, Pu) geometry.[6]

Results and Discussion

Syntheses

The lithium and ammonium salts of the tetraphenolic macrocyclic uranyl complexes $[A]_2[UO_2(TC4A)]$ (A = $HNEt_3$ **1-HNR3**; Li(DME) **1-Li**) were synthesized and fully characterized, see SI, Tables SI1-7, and Figure 1, following a modified literature preparation of **1-HNR3** in 58 and 43 % yield, respectively.[14a] SCXRD analysis (see Supporting Information Fig.S11–12) of **1-Li** shows *pseudo*-C_{2v} symmetry, as lithium cations are bound to pairs of the TC4A phenoxides, one S atom on each side of the complex, and capped by DME, as drawn in Figure 1. The cations in **1-HNR3** show a lower level of interaction, with hydrogen bonds to just two of the TC4A phenoxide O atoms, Figure 1 (Figure S17).[14a] No interaction with a uranium oxo is observed, in line with the low expected Lewis basicity of the uranyl oxo group.[1b] The ^1H and $^{13}C\{^1H\}$ NMR spectra show **1-Li** is *pseudo*-C_{4v} symmetric in C_6D_6 solution at room temperature (Figure S1–2). A single resonance is observed at 3.17 ppm in the ^7Li NMR spectrum of **1-Li**, significantly shifted from 0 ppm, indicating the Li cations are still bound to the molecule, but likely are moving between different pairs of ligand phenolate O atoms on the NMR spectroscopic timescale. The ^1H and $^{13}C\{^1H\}$ NMR spectra of **1-HNR3** also suggest a fluxional process involving the cations exchanging positions, and the gross features of the UO_2 macrocycle segment in all three complexes **1** are the same spectroscopically.

The solid-state FTIR spectrum shows multiple bands associated with ligand stretches in the window of interest for the actinyl asymmetric stretch. **1-Li** displays an absorption at 908 cm^{-1} assigned as $\nu_{asym}(O{=}U{=}O)$; this is a higher energy stretch than that observed for **1-NHR3** (887 cm^{-1}) (Figure S3–5), which we attribute to increased interaction of the TC4A phenoxides with lithium. Cyclic voltammetry studies of THF solutions of **1** showed no redox processes within the solvent window.

We were keen to target heavier, transuranic TC4A actinyl complexes, which would be the first to be desymmetrized in this way. Treatment of $AnO_2^{VI}(NO_3)_2(H_2O)_n$[17] (Np, Pu) with H_4TC4A and an excess of NEt_3 in DMSO affords yellow-orange microcrystalline $[HNEt_3]_2[NpO_2^{VI}(TC4A)]$ **1Np** and an orange-brown powder of $[HNEt_3]_2[PuO_2^{VI}(TC4A)]$ **1Pu** after workup (SI, Fig.S6–8 and Figure 1). **1Np** complex exhibits a strong, characteristic absorption in the UVvis spectrum at 514 nm and well-defined paramagnetic resonances in the ^1H NMR spectrum, which span a particularly narrow chemical shift range (1.78 to 0.94 ppm). **1Pu** exhibits a strong, characteristic absorption profile for Pu(VI) in the UV/Vis spectrum at 849, 970, 995, 1098 nm and similar to the neptunyl system, well-defined paramagnetic resonances in the ^1H NMR spectrum, which span the chemical shift range 1.78 to 0.94 ppm.[18] The solid-state Raman spectrum of **1Pu** shows the actinyl symmetric stretch at 723 cm^{-1}, which is substantially lower than the unligated $PuO_2^{VI}(NO_3)_2(H_2O)$ complexes (836, 844), in line with the substantial change in electron donation due to the coordinated TC4A ligand.[19]

Unfortunately, we were unable to grow crystals suitable for single crystal X-ray diffraction, but powder X-ray diffraction data for **1Np** confirm it is isostructural with **1-HNR3**.

DFT calculations were carried out on complexes **1U**, **1Np** and **1Pu** to better understand the bonding in these three actinyl complexes. The optimized geometry of the computed analogue of **1U**, denoted here as **1U'** compares

well with that of the experimental one. In particular, the U-O_{yl} bonds are well reproduced compared to the uranium crystal structures (1.78 and 1.79 Å vs. 1.78 and 1.79 Å experimentally) as well as the U-O_{TC4A} bonds (2.28 and 2.29 Å vs. 2.28 and 2.31 Å experimentally). This supports the correct choice of computational method. The bonding analysis was carried out with Natural Bonding Orbital (NBO) methods. As known since the late 1990's, the U-O_{yl} bonds are triple bonds strongly polarized toward O (80 %) involving overlap between either *sp* (σ) or pure *p* (π) orbitals on O and *df* (50–50) orbitals on U. This polarization of the bonds explains the U-O_{yl} Wiberg Bond Index (WBI) of 2.01. The U-O_{TC4A} interactions are described as single bonds that are even more strongly polarized toward O (94 %) involving overlap between one oxygen *sp* orbital and the U (with *s:d:f* orbital contributions in the ratio 20:30:40). The associated WBI are 0.58 in line with strongly polarized bonds. A similar analysis was carried out on **1Np'** and **1Pu'**. In both cases, the An - O_{yl} distances are slightly shorter than in the **1U'** analog (1.75/1.76 Å for Np and 1.74/1.74 Å for Pu). This slight decrease is in line with the actinide contraction. The NBO analysis indicates that the polarization toward O in the An–O_{yl} bonds decreases slightly with increasing nuclear charge (77 % for Np and 75 % for Pu). This is directly reflected by the Wiberg Bond Indices (WBI) for the An - O_{yl} bonds which increase slightly from U to Np to Pu (2.06 for Np and 2.08 for Pu); the 'yl' bonds thus show a slight increase in covalency with increasing nuclear charge. Mirroring these trends, the An-O_{TC4A} bonds are slightly shorter in **1Np'** and **1Pu'** than in **1-U'** (2.27 Å for both Np and Pu vs. 2.28/2.29 for U). However, the An – O_{TC4A} bonds are similar in the three cases with similar WBI of 0.58.

Reductive silylation and oxo migration of 1-HNEt3 and 1-Li

Treatment of **1-HNR3** with one equivalent of $(Me_3Si)_2pyz$ in tetrahydrofuran at room temperature (Scheme 1b) results in a rapid color change from yellow to green. Monitoring the reaction by ^1H NMR spectroscopy shows complete consumption of both reagents and concomitant ingrowth of pyrazine after 20 min, and no further changes in the mixture of paramagnetic products is observed by 2 h after mixing. Removal of volatiles then recrystallization from diethyl

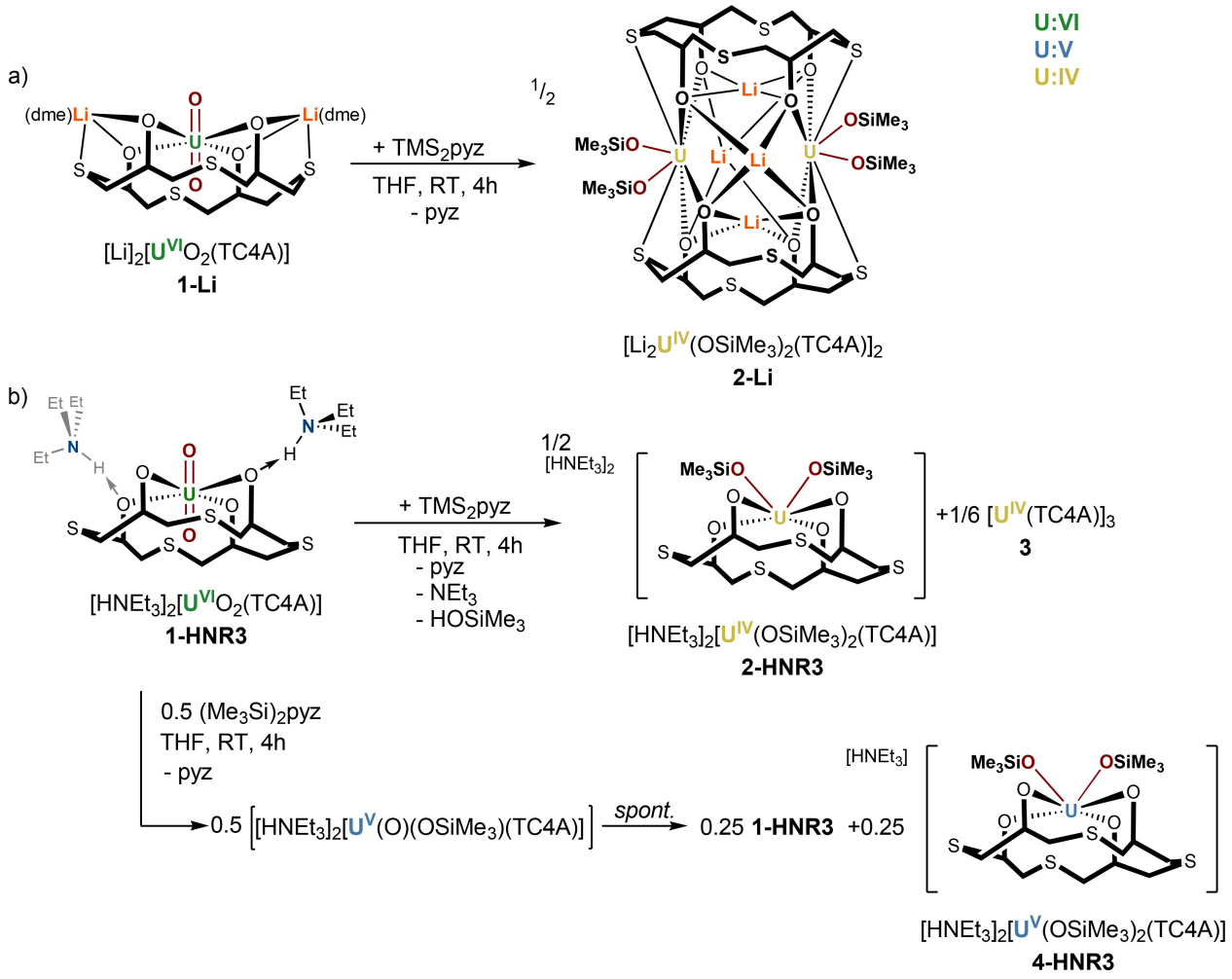

Scheme 1. Differences in the oxo-silylation and actinide reduction reactivity in complexes **1** depending on the identity of the cation A.

ether at −35 °C enables the isolation of two highly air-sensitive products, a green powder and blue crystals. The blue crystals were identified as $[U^{IV}(TC4A)]_3$, **3** via SCXRD (Figure S15–16). Based on computational and sub-stoichiometric reaction studies (see below), we identify the secondary (green species) as $[HNEt_3]_2[U^{IV}(OSiMe_3)_2(TC4A)]$, **2-HNR3**. The two are not separable due to their similar solubility (see SI). Complex **3** is formally formed from **2-HNR3** by the loss of $[HNEt_3][OSiMe_3]$. In the solid state it forms a trimer via O-bridging, resulting in a saturated uranium coordination sphere (see SI).

Treatment of **1-Li** with one equivalent of $(Me_3Si)_2$pyz in tetrahydrofuran at room temperature (Scheme 1a) results in a much slower reaction, with a gradual color change of the solution from yellow to blue-green, with full consumption of both reagents after 4 hours.

The oxo-silylated product $[Li_2U^{IV}(OSiMe_3)_2(TC4A)]_2$ **2-Li**, is isolated as a pale blue solid in 43 % yield. In **2-Li** the two oxo groups have migrated from *trans* to a *cis* conformation, and the two U centers now bridge across two calixarenes, forming a dimeric $U_2(TC4A)_2$ core via phenoxide bridging (Figure S13–14). Each uranium center thus binds two phenoxide O and two thioether S from different macrocycles. One lithium counter-cation binds symmetrically in each TC4A annulus (the original U site) and the other two bridge the two TC4As bind to four phenoxides on the open faces. Bond valence sum (BVS) analysis is consistent with a U^{IV} formal oxidation state (Table S1). A reaction to target the monosilylated complex, by treatment of $[HNEt_3]_2[U^{VI}O_2(TC4A)]$ with half an equivalent of $(Me_3Si)_2$pyz gave consumption of just half the starting material, but the reaction conditions favored the isolation of the doubly silylated U^V analogue of **2**, $[HNEt_3]$-$[U^V(OSiMe_3)_2(TC4A)]$ **4-HNR3** (Scheme 1b) which has been structurally characterized, see below.

The dc magnetic susceptibility data for the U^{IV} complex **2-Li** and U^V complex **4-HNR$_3$** under applied field of 0.1 T between 2 and 300 K (Figures S9 and S10) exhibit $\chi_m T$ of 1.45 K (after correction for impurity) and 0.65 K emu/mol at 300 K, respectively, which is slightly lower than the calculated values of 1.6 and 0.80 emu K/mol for one U^{4+} and U^{5+} ion.[20] Observing lower values than the theoretical values is common with both of these formal oxidation states. This is because their large magnetic anisotropy makes it difficult to complete thermal population of the M_J states, split by the crystal-fields, in the ground $^3H_4$ states for U^{4+} and in the ground $^2F_{5/2}$ states for U^{5+}, even at room temperature.[21] For both **2-Li** and **4-HNR$_3$** the $\chi_M T$ decreases as the temperature decreases to 2 K (**2-Li** = 0.039 emu K/mol, **HNR$_3$** = 0.064 emu K/mol). This drop at low temperature can be explained by thermal depopulation of the crystal-field excited M_J states.[22] Both **2-Li** and **4-HNR$_3$** were also tested for magnetic blocking,[23] but in each case only closed hysteresis was observed under these conditions.

Computational analysis of oxo-migration mediated by silylation

DFT calculations (B3PW91) including solvent and dispersion corrections were carried out to give some insights on the reactions reported in Scheme 1. Figure 2 displays the reaction mechanism calculated for **1-HNR3**. In THF, the calculation indicates that the counter-cations are readily displaced from the metal complex (exothermic by 9.2 kcal.mol^{-1}) so that the reaction is computed on the bare anion $[U^{VI}O_2(TC4A)]^{2-}$, denoted **1'**.

The reaction begins with the formation of a non-covalent interaction (NCI) between the $(Me_3Si)_2$pyz and the uranyl *exo* oxo group to form **Int1** (−8.2 kcal.mol^{-1}). This is exothermic because the interaction is very strong, and interestingly, much stronger than the sum of the hydrogen bonding interactions between the two $HNEt_3$ cations and the O atoms of the pairs of aryloxides in TC4A. From **Int1**, the silylation of the uranyl oxo occurs through transition state **TS1** with a barrier of 25.2 kcal.mol^{-1}, lower than for the Li congener below and in agreement with the more rapid reaction observed experimentally for **1-HNR3**. **TS1** was located on the singlet spin state potential energy surface (PES) and looks like the transition state for a nucleophilic substitution in which the silyl group is transferred as an electrophilic radical from the pyrazine to the oxo. However, a spin crossover occurs along the intrinsic reaction coordinate to lead to the adduct **Int2**, which is on the triplet spin state PES; its formation is exothermic by 16.9 kcal.mol^{-1}. The unpaired spin density plot for **Int2** (Figure 3) clearly indicates that reduction of the uranium center to U(V) has occurred and shows the presence of a radical on the (Me_3Si)pyz. Therefore, the first silylation is best described as reductive abstraction of a silyl radical by the uranyl.

It is also interesting to note that in **Int2** there is an NCI between the silyl group of the pyrazine radical formed in the previous step and the oxygen atom of the phenoxy groups present in the TC4A ligand. This NCI weakens the strength of the TC4A ligand so that a long-range, non-bonding interaction between the (Me_3Si)pyz radical and the remaining *endo*-oxo is even observed at the second order donor-acceptor level. This Van der Waals interaction is the driving force for the migration of the uranyl oxo from the *trans* to the *cis* position, bringing it out of the TC4A cavity, to yield **Int3** which has a stronger interaction between the (Me_3Si)pyz Si radical and the oxo, and is thus further stabilized by 2.6 kcal.mol^{-1} compared to **Int2**.

Then **Int3** readily abstracts the second silyl radical from the $[(Me_3Si)pyz]\bullet$ via **TS2** with a very low barrier of 2.2 kcal.mol^{-1}. **TS2** is very similar to **TS1** and is also a reductive abstraction of a silyl radical. After a second and final $Me_3Si\bullet$ abstraction the intrinsic reaction coordinate yields the very stable U(IV) product **2**, whose oxidation state is confirmed by the unpaired spin density of 2 calculated at the uranium center (Figure 3).

Mechanistic investigations were also carried out on the reaction with **1-Li**. First, the calculation does not indicate any displacement of the lithium counterion, in agreement with experimental observations (Figure 4).

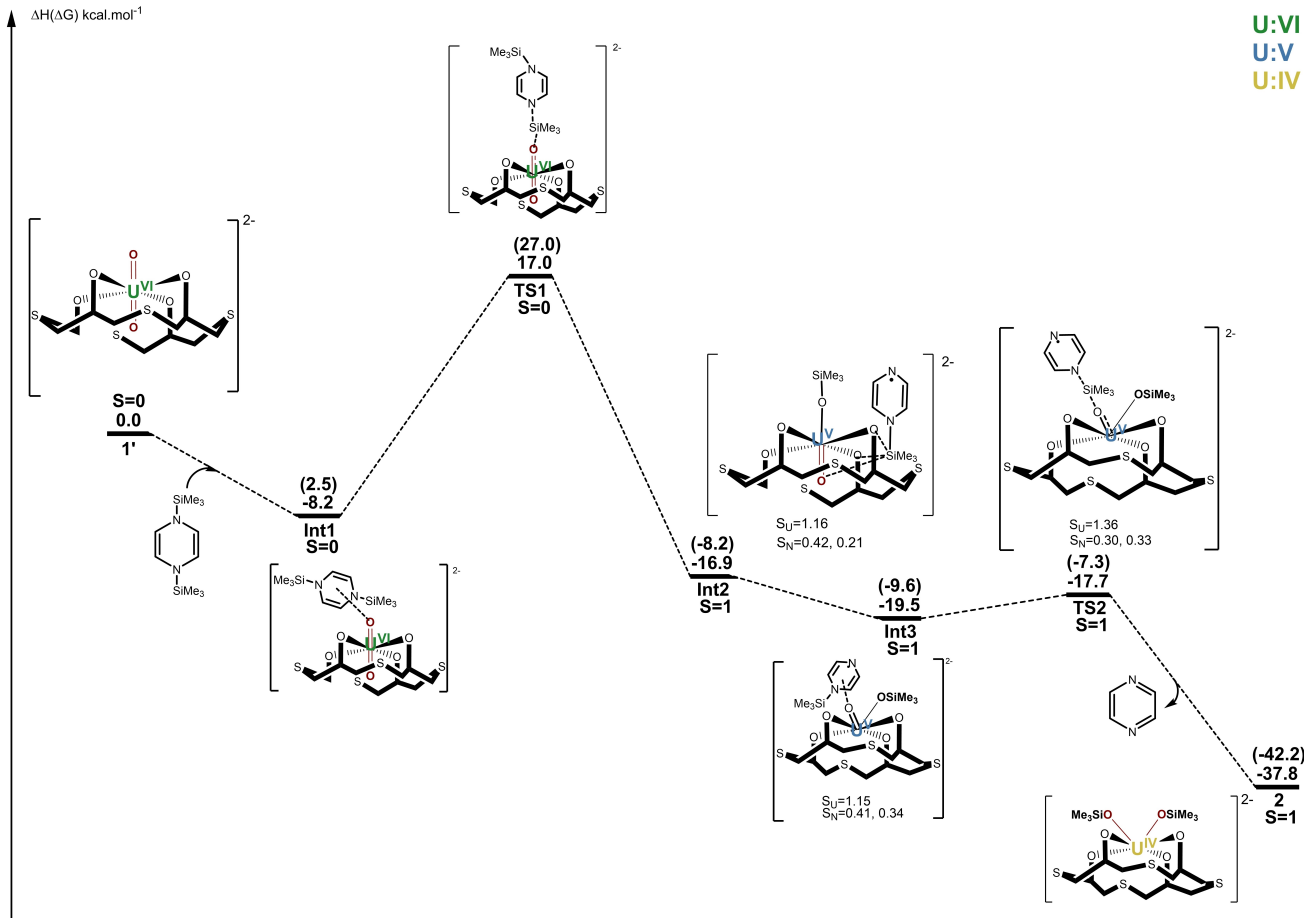

Figure 2. Computed mechanism for the silylation of **1'** (the dianion of **1-HNR3**) with $(Me_3Si)_2$pyz in THF solvent. The enthalpies are given at room temperature and the Gibbs Free energy between brackets. S_U and S_N are the unpaired spin densities.

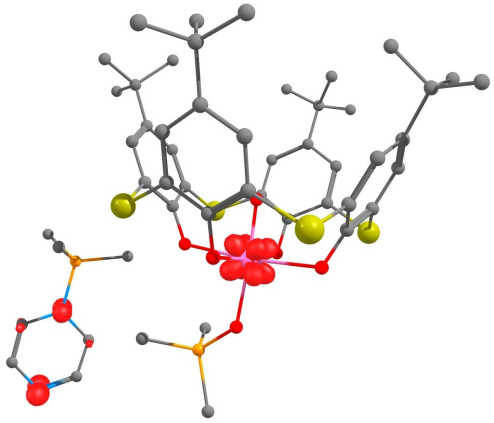

Figure 3. Unpaired spin density plot of the intermediate **Int2** showing the formal oxidation state is now U^V and the unpaired electron spin density on the [(Me_3Si)pyz]• fragment after loss of one $SiMe_3$ group.

The calculations find a first intermediate **Int1-Li2** in which there is a stabilizing interaction between the exo-oxo group and one $SiMe_3$ group of the pyz$(SiMe_3)_2$, Figure 4. The next step of the reaction starts to deviate from previous observations of the reductive silyl radical abstraction by an oxo group.[3b] The barrier for this abstraction is 34.1 kcal.mol^{-1}

The coordination of the lithium cation to the TC4A oxygen atoms in the equatorial plane rigidifies the structure, and hampers the formation of the NCI between the silyl group of the pyrazine radical and the oxygen of the phenoxy ligand of TC4A group in **Int2-Li2**, which facilitated the oxo migration and second O–Si bond formation in **1-HNR3** above. Instead, an NCI is observed between the phenyl ring of the pyrazine radical and the silyl group of the exo O-$SiMe_3$.

At this point, it is more favorable for the activated [(Me_3Si)pyz]• to react with another molecule of **1-Li**, forming a second equivalent of **Int2-Li2**. At this point, it is proposed that two molecules of **Int2-Li2** dimerize to form **Int3-Li2** since this is highly exothermic (−149.9 kcal.mol^{-1}) but demands the rearrangement of the Li atoms (to avoid electrostatic repulsion between them). This rearrangement releases the constraint imposed by the Li atoms on the TC4A ligand and induces the migration of the uranyl *endo*-oxo into the *cis* position. This dimer will react with another molecule of $(Me_3Si)_2$pyz to ultimately form **2-Li**, whose formation is very exothermic (−226.9 kcal.mol^{-1}). Due to

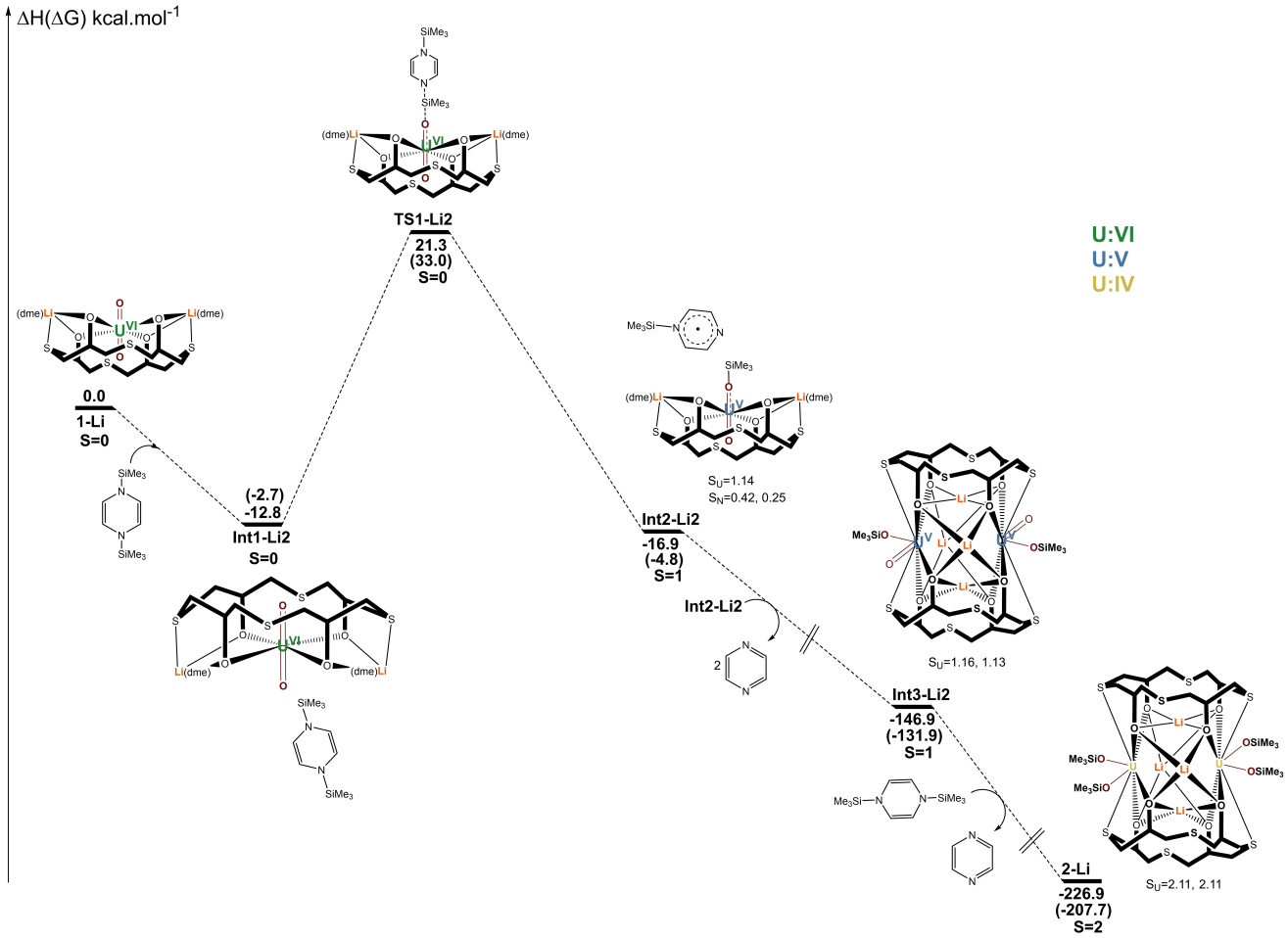

Figure 4. Computed mechanism for the silylation of **1-Li** with $(Me_3Si)_2$pyz in THF, in which the first oxo silylation enables the *endo* oxo migration to occur, forming a Li-stabilized intermediate which dimerizes prior to the second oxo-group silylation forming the *cis*(siloxide) geometry in **2-Li**. The enthalpies are given at room temperature and the Gibbs Free energy between brackets. S_U are the unpaired spin densities.

the size of these dimeric complexes, it was not possible to locate any TS for the reactions.

Molecular and electronic structures of the cis-siloxides and a computed cis-dioxo actinyl product

Single crystal X-ray diffraction (SCXRD) data for **1-Li** are described and compared with **1-HNR3** in the SI. The molecular structure of the U^V complex **4-HNR3** (single crystal X-ray diffraction data, Figure 5) shows the flattening of the TC4A macrocycle that stabilizes the *cis*-$(OSiMe_3)_2$ moiety, while the one remaining A counter-cation still forms an H-bonding interaction with one TC4A phenoxide.

As mentioned above, the dianion in the uranium (IV) complexes **2** is computed as a triplet ground state with the unpaired spin density fully localized at the uranium center, in line with a U(IV) formal oxidation state, Figure 6a. A similar conclusion is drawn from scrutinizing the Molecular Orbitals (MO) since the two SOMOs (see SI) are two pure f orbitals. A Natural Bonding Analysis of this complex indicates the presence of single U–O bonds which are strongly polarized toward O (92 %). The U–O Wiberg Bond Indexes (WBI) are 0.76 indicating that these bonds have a strong donor-acceptor character.

The possibility of isolating a *cis* dioxo U^{VI} uranyl complex was explored computationally, which would be a new geometry for the ubiquitous uranyl ion, and of academic interest to compare actinides with the group 6 d-block M^{VI} cations which favor the *cis*-MoO_2 and WO_2 geometries. The calculations show that **1U-cis**, Figure 6b, would be a stable structure if it could be accessed synthetically, at only 23 kcal.mol^{-1} less stable than the classical *trans* dioxo isomer **1U**. The optimized geometry found for **1U-cis** is somewhat different from that found for **1** in particular with respect to the TC4A macrocycle. **1U-cis** is still *pseudo*-octahedral but the TC4A macrocycle has flattened from the conical shape in order to facially cap the U^{VI} center. The two aryloxides *trans* to the two oxo groups, O8 and O9, bend to create a shallower U–O–C_{Ar} to place the two O_{Ar} atoms in a mutually *cis* configuration while the other two aryloxides, O6 and O7, remain in the geometry closer to the previously observed cone.

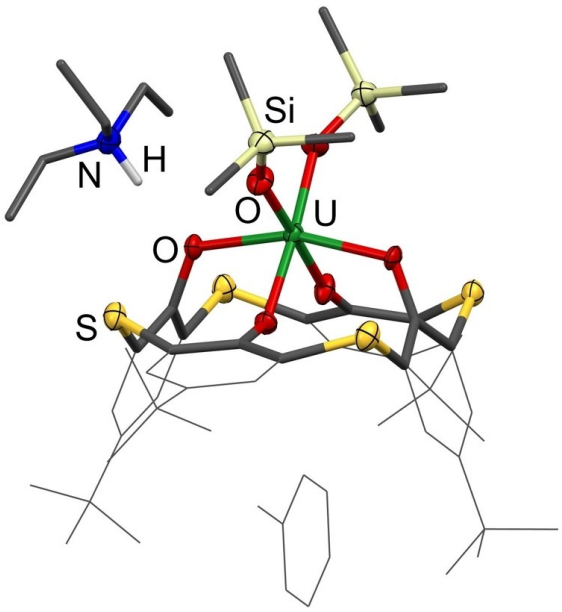

Figure 5. Molecular structure of **4-HNR3**, displacement ellipsoids at 50%, peripheral atoms shown wireframe, H atoms and lattice solvent omitted for clarity.

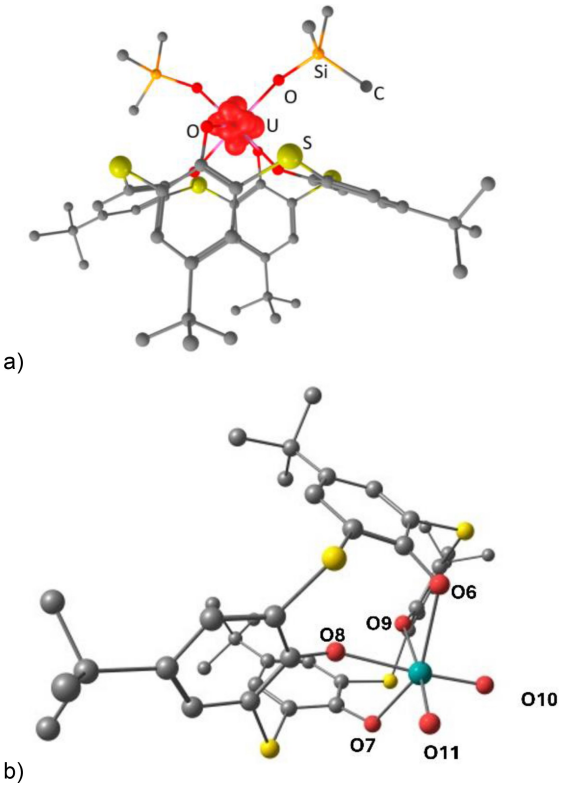

Figure 6. a) Computed unpaired spin density of the dianionic *cis*-disiloxide **2-HNR3**, with H omitted for clarity. b) computed geometry of the U^{VI} *cis*-dioxo **1-cis** that would be generated by oxidative desilylation of **2**.

It is interesting to note the differences in the U-oxo bonding in **1U-cis** compared to that found for **1U**. The two $U\text{-}O_{yl}$ bonds are found to be triple bonds polarized toward O (77 to 80%) as found for **1U** (see SI). However, the $U\text{-}O_{yl}$ bond lengths in **1U-cis** are longer, at 1.82 Å, compared with 1.78 and 1.79 Å in **1U**. These bonds are slightly more covalent in **1U-cis** than in **1U** (U–O WBI of 2.07 in **1U-cis** vs. 2.01 in **1**) while the ionic contribution to the bonding still dominates, and perhaps more so for the *trans* isomer. The frontier orbitals are also similar in these two complexes (see ESI).

The possibility to access the related, and as yet unknown, *cis* dioxo transuranic cations $[HNEt_3]_2[cis\text{-}AnO_2(TC4A)]$, **1Np-cis** and **1Pu-cis** were also investigated computationally. Unfortunately, in both cases, the stability of the *cis* isomer is 30 to 36 $kcal.mol^{-1}$ less stable than the *trans* isomer, that is even less favorable than in the uranyl case.

Interestingly, the U-aryloxide bonding is different in the *cis* isomer. In **1U**, all four U–O bonds are strongly polarized toward O (94%) with some covalent character suggested by the WBI of 0.6. In **1U-cis**, the $U\text{-}O_{axial}$ are similar to that found in **1U** (polarized U–O bond toward O (94%)) while the two $U\text{-}O_{Ar}$ that are *trans* to the oxos have double bond character, while still containing a strong polarization to O (90%). The additional bonding in these two $U\text{-}O_{Ar}$ bonds stabilizes the two U=O yl bonds, explaining the stability of **1U-cis** in this ligand framework. The latter is highlighted by the two $U\text{-}O_{Ar}$ WBI that are increased to 0.68 in **1U-cis** while the two other $U\text{–}O_{axial}$ WBI are decreased to 0.48. This accounts for the difference of stability of the **1U-cis** complex with respect to **1U**. We therefore computed the possibility of thermally converting **2** to **1U-cis** and releasing the disilane $Me_3Si\text{-}SiMe_3$ but this reaction is predicted to be too energetically demanding (more than 80 $kcal.mol^{-1}$) to be performed thermally. Experimentally, reactions with silver salts, aimed at oxidative desilylation were unsuccessful in removing the silyl groups, and resulted in oxidation of the metal center to the U(V) species, and we suggest that a photochemically driven oxidation would be most likely to succeed. It is hard to predict from the calculations how we should electronically modify the ligand in order to retain the *cis* geometry upon re-oxidation, but we suggest that a stronger donor in the equatorial plane is the most likely route to success. As found in the **1U-cis** case, the $An\text{-}O_{yl}$ bonds in **1Np-cis** and **1Pu-cis** are found to be slightly more covalent than in the trans isomer (WBI of 2.15 vs. 2.06 for Np and WBI 2.13 *vs.* 2.08 for Pu) with bonds polarized toward O (70–76% for Np, 63–73% for Pu). As already found in **1U-cis**, the $An\text{-}O_8$ and $An\text{-}O_9$ bonds that are *trans* to the $An\text{–}O_{yl}$ in **1Np-cis** and **1Pu-cis** exhibit a double character strongly polarized toward O (90%). Further, also as in **1U-cis**, the $An\text{-}O_{axial}$ WBI in **1Np-cis** and **1Pu-cis** indicates that the two $An\text{-}O_{TC4A}$ that are *trans* to the $An\text{-}O_{yl}$ ligands are slightly more covalent than in **1An** (0.70 for Np and 0.68 for Pu) while the two remaining oxos are slightly less covalent (0.47 for Np and 0.57 for Pu). This again accounts for the difference in stability of the two isomers.

Conclusion

To conclude, new actinyl complexes of the TC4A tetraphenolate macrocycle are air-stable and the counter-cations play an essential role in the activation and silylation of uranyl TC4A complexes. To our knowledge, this is the first time that the neptunyl and plutonyl oxo groups have been differentiated in a molecule, and the air-stability of these desymmetrized actinyl ions should help to enable the study of single oxo chemistry of the transuranic actinyl cations. Silylation of the dilithium salt **1-Li**, whose counter-cations bind to the complex at two of the TC4A oxygen atoms and one S atom, occurs more slowly than silylation of the literature reported **1-HNR3** whose counter-cations show a hydrogen bonding interaction with the same phenoxides that is a little weaker. Calculations show that after the first oxo silylation, van der Waals bonding between the (Me_3Si)pyz radical and the remaining oxo (**Int2**) drives the migration of the uranyl oxo from the *trans* to the *cis* position in the U^V intermediate, prior to the second oxo silylation, and the flexibility of the TC4A ligand facilitates this rearrangement. According to theory, the flexibility of the TC4A ligand is also useful in providing two O donors in mutually *trans* positions that can stabilize a putative *cis* dioxo U^{VI} uranyl complex, **1U-cis**. This would be a new geometry for the ubiquitous uranyl ion, and is predicted to be only 23 kcal.mol^{-1} less stable than the classical *trans* dioxo isomer **1U** in this ligand frame if it could be accessed synthetically. Calculations on the as-yet-unseen **1Np-cis** and **1Pu-cis** analogues show them to be less stable than **1U-cis** but that the TC4A framework again generates an environment in which the ligand O atoms that are *trans* to the An=O bonds have more double bond character, and slightly higher covalent character, which increases in the order **1U-cis** < **1Np-cis** < **1Pu-cis**. We suggest that functionalization of the TC4A to provide a stronger equatorial ligand field could help to increase the accessibility of a stable $[cis\text{-}AnO_2]^{2+}$ ion geometry. Finally, the U–O bonding in **1U-cis** is slightly more covalent than that in **1** for all three actinides. Work is in progress to modify the TC4A ligand to target this, and to explore the transuranic oxo-silylation chemistry.

Supporting Information

Additional experimental, computational, and crystallographic data (PDF). Crystallographic datasets are available from the CCDC deposition numbers CCDC2404473-2404476. Open data are available at https://doi.org/10.5061/dryad.bcc2fqzpn. The authors have cited additional references within the Supporting Information: six synthetic and six computational [24–36].

Acknowledgements

The synthetic parts of this research were supported by the Heavy Element Chemistry Program (synthetic work) and the Molecular Qubits Project of the Quantum Information Science program of the U.S. DOE, Office of Science, Basic Energy Sciences, CSGB Division under contract DE-AC02-05CH11231. R.L.M., S.G.M., and the spectroscopic component of this work were supported by the Quantum Information Sciences program of the aforementioned Division of the U.S. DOE under Contract No. DE-AC02-05CH11231.We would like to acknowledge Dr. Joshua Woods for help with some of the synthetic aspects and Dr Megan R. Keener for help with the Pu spectroscopy. This material is based upon some synthetic uranyl chemistry supported by the National Science Foundation MPS-Ascend Postdoctoral Research Fellowship under Grant No. 2213284, and upon work supported under a Department of Energy Nuclear Energy University Programs Graduate Fellowship (DF and CSC).

Conflict of Interest

The authors declare no conflict of interest.

Data Availability Statement

The data that support the findings of this study are available in the supplementary material of this article, and in the open data archive on Mendeley DOI: 10.17632/np7xzfrfxd.1.

Keywords: actinides · electronic structure · ligand effects · transuranium elements

[1] a) J. C. Renshaw, L. J. C. Butchins, F. R. Livens, I. May, J. M. Charnock, J. R. Lloyd, *Environ. Sci. Technol.* **2005**, *39*, 5657–5660; b) B. E. Cowie, J. M. Purkis, J. Austin, J. B. Love, P. L. Arnold, *Chem. Rev.* **2019**, *119*, 10595–10637; c) C. Hopkins, H. Simmonds, J. Cryer, D. Moulding, D. L. Jones, S. Randall, L. S. Natrajan, in *Handbook on the Physics and Chemistry of Rare Earths Vol. 66*, Elsevier, **2024**, p. 231.

[2] a) B. E. Cowie, I. Douair, L. Maron, J. B. Love, P. L. Arnold, *Chem. Sci.* **2020**, *11*, 7144–7157; b) G. M. Jones, P. L. Arnold, J. B. Love, *Chem. - Eur. J.* **2013**, *19*, 10287–10294; c) R. J. Baker, *Chem. Eur. J.* **2012**, *18*, 16258–16271; d) S. Fortier, T. W. Hayton, *Coord. Chem. Rev.* **2010**, *254*, 197–214; e) P. L. Arnold, D. Patel, C. Wilson, J. B. Love, *Nature* **2008**, *451*, 315–317.

[3] a) A. Kumar, D. Lionetti, V. W. Day, J. D. Blakemore, *J. Am. Chem. Soc.* **2020**, *142*, 3032–3041; b) P. L. Arnold, A.-F. Pécharman, R. M. Lord, G. M. Jones, E. Hollis, G. S. Nichol, L. Maron, J. Fang, T. Davin, J. B. Love, *Inorg. Chem.* **2015**, *54*, 3702–3710.

[4] K. Liu, X. Chi, Y. Guo, K. Hu, L. Mei, J. Yu, W. Shi, *New J. Chem.* **2024**.

[5] G. Schreckenbach, P. J. Hay, R. L. Martin, *Inorg. Chem.* **1998**, *37*, 4442–4451.

[6] T. W. Hayton, *Dalton Trans.* **2018**, *47*, 1003–1009.

[7] H. Oher, A. S. P. Gomes, R. E. Wilson, D. D. Schnaars, V. Vallet, *Inorg. Chem.* **2023**, *62*, 9273–9284.

[8] S. Schöne, T. Radoske, J. März, T. Stumpf, M. Patzschke, A. Ikeda-Ohno, *Chem. Eur. J.* **2017**, *23*, 13574–13578.

[9] a) P. L. Arnold, A.-F. Pécharman, J. B. Love, *Angew. Chem. Int. Ed.* **2011**, *50*, 9456–9458; b) V. Mougel, P. Horeglad, G.

Nocton, J. Pécaut, M. Mazzanti, *Chem. Eur. J.* **2010**, *16*, 14365–14377.
[10] a) N. L. Bell, B. Shaw, P. L. Arnold, J. B. Love, *J. Am. Chem. Soc.* **2018**, *140*, 3378–3384; b) D. D. Schnaars, G. Wu, T. W. Hayton, *Inorg. Chem.* **2011**, *50*, 4695–4697.
[11] a) P. L. Arnold, D. Patel, A. J. Blake, C. Wilson, J. B. Love, *J. Am. Chem. Soc.* **2006**, *128*, 9610–9611; b) P. L. Arnold, E. Hollis, F. J. White, N. Magnani, R. Caciuffo, J. B. Love, *Angew. Chem., Int. Ed.* **2011**, *50*, 887–890; c) B. E. Cowie, G. S. Nichol, J. B. Love, P. L. Arnold, *Chem. Commun.* **2018**, *54*, 3839–3842.
[12] a) P. L. Arnold, G. M. Jones, S. O. Odoh, G. Schreckenbach, N. Magnani, J. B. Love, *Nat. Chem.* **2012**, *4*, 221; b) P. L. Arnold, G. M. Jones, S. O. Odoh, G. Schreckenbach, N. Magnani, J. B. Love, *Nat. Chem.* **2012**, *4*, 221–227.
[13] P. L. Arnold, E. Hollis, G. S. Nichol, J. B. Love, J.-C. Griveau, R. Caciuffo, N. Magnani, L. Maron, L. Castro, A. Yahia, S. O. Odoh, G. Schreckenbach, *J. Am. Chem. Soc.* **2013**, *135*, 3841–3854.
[14] a) Z. Asfari, A. Bilyk, J. W. C. Dunlop, A. K. Hall, J. M. Harrowfield, M. W. Hosseini, B. W. Skelton, A. H. White, *Angew. Chem. Int. Ed.* **2001**, *40*, 721–723; b) I. V. Khariushin, V. Bulach, S. E. Solovieva, I. S. Antipin, A. S. Ovsyannikov, S. Ferlay, *Coord. Chem. Rev.* **2024**, *513*, 215846.
[15] V. K. Nikolova, C. V. Kirkova, S. E. Angelova, T. M. Dudev, *Beil. Org. Chem.* **2019**, *15*, 1321–1330.
[16] L. R. Valerio, B. M. Hakey, W. W. Brennessel, E. M. Matson, *Chem. Commun.* **2022**, *58*, 11244–11247.
[17] P. Lindqvist-Reis, C. Apostolidis, O. Walter, R. Marsac, N. L. Banik, M. Y. Skripkin, J. Rothe, A. Morgenstern, *Dalton Trans.* **2013**, *42*, 15275–15279.
[18] A. J. Gaunt, I. May, M. P. Neu, S. D. Reilly, B. L. Scott, *Inorg. Chem.* **2011**, *50*, 4244–4246.
[19] M. Autillo, R. E. Wilson, M. Vasiliu, G. F. de Melo, D. A. Dixon, *Inorg. Chem.* **2022**, *61*.
[20] R. Skomski, *Simple models of magnetism*, Oxford university press, **2008**.
[21] E. J. Schelter, P. Yang, B. L. Scott, J. D. Thompson, R. L. Martin, P. J. Hay, D. E. Morris, J. L. Kiplinger, *Inorg. Chem.* **2007**, *46*, 7477–7488.
[22] a) C. R. Graves, A. E. Vaughn, E. J. Schelter, B. L. Scott, J. D. Thompson, D. E. Morris, J. L. Kiplinger, *Inorg. Chem.* **2008**, *47*, 11879–11891; b) S. J. Kraft, U. J. Williams, S. R. Daly, E. J. Schelter, S. A. Kozimor, K. S. Boland, J. M. Kikkawa, W. P. Forrest, C. N. Christensen, D. E. Schwarz, P. E. Fanwick, D. L. Clark, S. D. Conradson, S. C. Bart, *Inorg. Chem.* **2011**, *50*, 9838–9848; c) F. Delano, S. Demir, *Chem* **2021**, *7*, 1686–1688; d) J. T. Boronski, J. A. Seed, D. Hunger, A. W. Woodward, J. van Slageren, A. J. Wooles, L. S. Natrajan, N. Kaltsoyannis, S. T. Liddle, *Nature* **2021**.
[23] K. R. Meihaus, J. R. Long, *Dalton Trans.* **2015**, *44*, 2517–2528.

Manuscript received: November 25, 2024
Accepted manuscript online: January 21, 2025
Version of record online: ■■, ■■

Research Article

Actinides

M. M. Pyrch, R. L. Meyer, T. Rajeshkumar, P. A. Cooke, D. J. Fiszbein, E. Ito, N. J. Katzer, C. S. Conour, S. G. Minasian, L. Maron, P. L. Arnold.* e202422974

Ligand-Directed Actinide Oxo-Bond Manipulation in Actinyl Thiacalix[4]arene Complexes

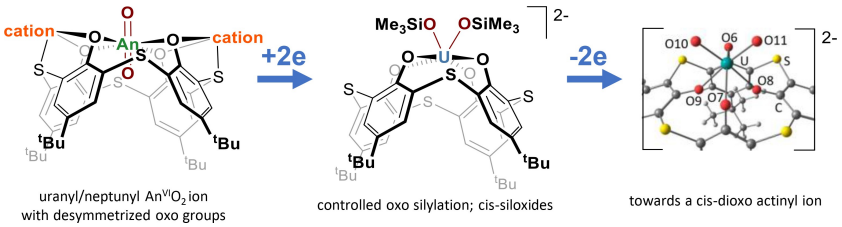

uranyl/neptunyl $An^{VI}O_2$ ion with desymmetrized oxo groups

controlled oxo silylation; cis-siloxides

towards a cis-dioxo actinyl ion

Thioether – expanded calixarene actinyl ions $[UO_2]^{2+}$, $[NpO_2]^{2+}$ and $[PuO_2]^{2+}$ place the two *trans*-oxo groups in different environments. One is more accessible, so functionalization and redox reactions are explored to target a *cis*-dioxo uranyl ion. Calculations confirm that only one silylation event is needed to initiate oxo rearrangement, and that the putative *cis* dioxo isomer of $[UO_2(TC4A)]^{2-}$ would be stable if it could be accessed synthetically.